

Towards Stochastic Deep Convective Parameterization

Johnny Wei-Bing Lin and J. David Neelin

*University of Chicago, Department of the Geophysical Sciences
5734 S. Ellis Ave., Chicago, IL 60637, USA
jlin@geosci.uchicago.edu*

ABSTRACT

Convective parameterizations used in general circulation models (GCMs) generally only simulate the mean or first-order moment of convective ensembles and do not explicitly include higher-order moments. The influence of including unresolved higher-order moments is investigated using stochastic deep convective parameterization. Two classes of parameterization are described: “empirical” schemes that directly control the distribution of heating to match observations, and “physics-motivated” schemes where the stochastic component is introduced into the existing parameterization framework, motivated by the physics of unresolved moments. Impacts are tested in an tropical atmospheric model of intermediate complexity as well as a comprehensive GCM. Adding convective noise noticeably affects tropical intraseasonal variability, suggesting inclusion of such noise in GCMs might be beneficial. Model response to the noise is sensitive not only to the noise amplitude, but also to such particulars of the stochastic parameterization as autocorrelation time and interaction with model dynamics.

1 Introduction

In the atmosphere, it is reasonable to hypothesize that for a given large-scale temperature and moisture field, there is a contribution to the variability of convection that arises inherently from small-scale motions, but which are not well represented by large ensemble means. Though this process has relatively short correlation scales in both time and space, it can act as a noise forcing that potentially shows up at the large-scales. Very little is understood, however, about the extent to which this hypothesis may be true.

In order to help quantify the importance of representing deviations from the ensemble mean, and as an alternative to a deterministic method of quantifying the importance of unresolved variance, we suggest that stochastic convective parameterizations can be developed for general circulation models (GCMs) that explicitly include the effects of the higher-moments of convection. We propose that methods of including unresolved variance through a stochastic parameterization may be grouped into two general approaches or classes:

“Empirical” schemes. Directly controlling the statistics of the overall convective heating by specifying a distribution as a function of model variables, with this dependence estimated empirically.

“Physics-motivated” schemes. Stochastic processes introduced within the framework of the convective parameterization, informed by at least some of the physics that contribute to unresolved variance.

An important difference between the two is that in “physics-motivated” schemes, the distribution (of such quantities as precipitation, days of zero precipitation, etc.) is not known in advance and is determined by interactions of the stochastic process with both the other elements of the convective parameterization and with the large-scale dynamics. In “empirical” schemes there is an implicit assumption that the distribution, e.g. of precipitation, is sufficiently independent of interactions with the large-scale such that it is reasonable to

estimate outside the model framework, and thus can be calibrated offline. It is not clear in advance which approach is likely to be more fruitful, and so we endeavor to set up and test examples of each.

In the present work, four examples of the above two approaches are described. The first example is an implementation of the “empirical” approach, and is called the “empirical lognormal” scheme. In this example scheme variance is added by tailoring the convective heating so that it reproduces certain statistical properties derived from observations. This type of empirically derived parameterization is similar in ways to the point process models (e.g. [Eagleson 1978](#)) used in hydrology to represent temporal rainfall, while reproducing selected statistical properties. The “empirical lognormal” stochastic convective parameterization is implemented in a tropical atmospheric model of intermediate-level complexity.

The last three examples are implementations of the “physics-motivated” approach. In the first two examples, the CAPE-based framework of the existing convective parameterization of an atmospheric model is modified by adding a zero mean, red noise forcing term. This is tested in a Betts-Miller ([1986](#))-type parameterization in an intermediate-level atmospheric model and in a Zhang-McFarlane ([1995](#)) plume ensemble scheme in a comprehensive GCM. The former is called the “CAPE scheme” while the latter is called the “CAPE- M_b scheme.” In the final test we examine simple stochastic perturbations to the vertical structure of heating in the Zhang-McFarlane deep convective scheme of a comprehensive GCM. This is called the “VSH scheme.”

The research summarized in the present study is described in [Lin and Neelin \(2000, 2002, 2003\)](#). See those references for details regarding the models and data used, analysis methods, and results (except for the lag-regression plots).

2 Models and Data

Two models are used in the present study: a tropical atmospheric model of intermediate-level complexity and a comprehensive GCM. For both models, climatological sea surface temperatures are prescribed. The [Spencer \(1993\)](#) daily precipitation estimates, calculated from passive radiometer measurements by the microwave sounding unit (MSU) carried on the TIROS-N and NOAA series of polar orbiting satellites, are used for observed precipitation.

The intermediate-level model used is version 2.1 of the Neelin-Zeng Quasi-Equilibrium Tropical Circulation Model (QTCM1), a primitive equation-based atmospheric model that focuses on simulating the tropical atmosphere. The QTCM1 uses a Galerkin expansion in the vertical to obtain a highly-truncated set of basis functions consistent with convective quasi-equilibrium conditions. The QTCM1 is more complex than a simple model, and includes full primitive equation nonlinearity and a radiative-convective feedback package. Being simpler than a full-scale GCM, the QTCM1 is easier to diagnose and is computationally faster. The QTCM1 uses the Betts-Miller moist convective adjustment scheme ([Betts and Miller 1986](#)), a scheme that is also used in some GCMs. Horizontal grid size is 5.625° in longitude and 3.75° in latitude. For a full description of model formulation (for v2.0), see [Neelin and Zeng \(2000\)](#); [Zeng et al. \(2000\)](#) provides initial results of the model (using v2.1).

The comprehensive GCM used is the NCAR CCM3 ([Kiehl et al. 1998](#)). This spectral GCM has a comprehensive suite of parameterizations, including convection, clouds, radiation, and the atmospheric boundary layer, and is coupled to the LSM v1.0 land-surface model of [Bonan \(1998\)](#). Deep convection is described by the Zhang-McFarlane scheme ([Zhang and McFarlane 1995](#)), hereafter ZM) which represents sub-grid convection by an ensemble of quasi-steady updrafts and downdrafts. Horizontal spectral truncation is T42 (approximately $2.8^\circ \times 2.8^\circ$ longitude-latitude) and 18 vertical levels are used, with a 20 min time step.

3 “Empirical” Schemes

3.1 The QTCM1 Empirical Lognormal Scheme

Being a highly nonlinear process, a full statistical characterization of precipitation requires consideration of a variety of measures. In the present study we focus on simulating two relatively gross statistical measures: precipitation variance and distribution of precipitation (including the percentage of time precipitation equals zero). We hypothesize that much of the sub-grid scale variance that shows itself at the grid scale will be high-frequency and low magnitude. At the same time, we aim to preserve the mean precipitation simulated by the model.

In the empirical lognormal scheme the results of the Betts-Miller calculated precipitation is used as input into a stochastic convection generator, which uses an empirically determined probability distribution to yield the value of precipitation that is seen by the model’s prognostic temperature and moisture equations. Following [Kedem et al. \(1990\)](#), precipitation is modeled in this study as following a mixed lognormal distribution, where non-zero intensities are described by a continuous lognormal distribution, and zero intensity is described by a discrete impulse probability. In order to simulate the effects of varying the autocorrelation timescale of convection, the randomly chosen convection is embedded in an autoregressive scheme.

Runs are made at different autoregressive characteristic timescales ($\tau_\xi = 20$ min, 2 hrs, and 1 day). Model runs are also conducted both with and without model dynamics. Finally, sensitivity tests are conducted by multiplying the randomly chosen convective heating Q_c by a factor α . Details of the scheme are described in [Lin and Neelin \(2002\)](#).

Figure 1 shows wavenumber 1 spectral power for 850 hPa zonal wind in an equatorial band, for the three τ_ξ cases and $\alpha = 1$. The addition of stochastic noise produces noticeable effects on eastward propagating intraseasonal variability, with preferential enhancement of lower frequency variability. Higher values of τ_ξ generally produce higher levels of intraseasonal variability spectral power. The westward peak seen in wavenumber 1 spectral power is due to aliasing of the annual cycle (also in Figure 4).

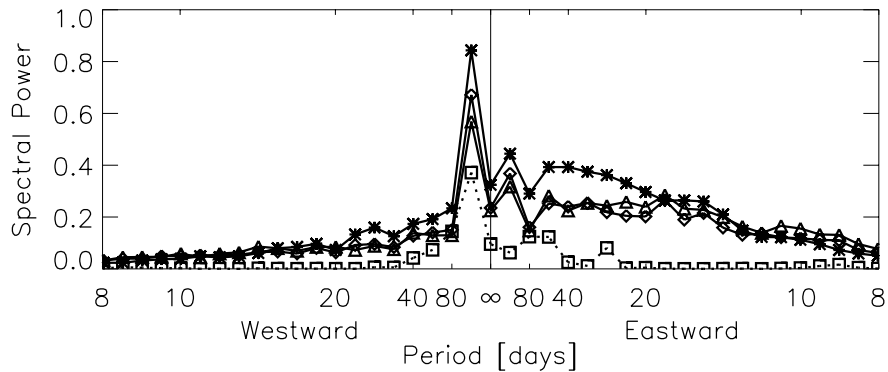


Figure 1: 850 hPa zonal wind spectral power of daily mean anomalies for wavenumber 1 in an equatorial band from 5.625°N – 5.625°S . Runs are shown for τ_ξ equals 20 min (triangle), 2 hrs (diamond), and 1 day (asterisk). A control run with deterministic Q_c is shown by the dotted line (square). Units of power are $(\text{m s}^{-1})^2$. Standard deviation of the spectral power estimator is 10%.

Figure 2 shows January precipitation climatology for the control run and the empirical lognormal scheme with $\tau_\xi = 1$ day for $\alpha = 1$ and $\alpha = 11$. Compared with the control run, the climatology for the stochastic cases

are similar, even though in the two cases the value of α differs by a factor of 11. Model feedbacks appear to decrease the sensitivity of climatology to the stochastic parameterization. Additionally, for the $\alpha = 11$ case, the presence or absence of model dynamics (not shown) appears to have little affect on climatology. In all, climatology appears to be fundamentally determined by large-scale model processes. The climatology of the system tends towards a state that is set by the choice of parameters unrelated to the presence of stochastic noise; stochastically driven variations in the presence of nonlinearity is of secondary importance in setting the mean state.

4 “Physics-motivated” Schemes

4.1 The QTCM1 CAPE Scheme

The QTCM1’s default convective parameterization is a simplified Betts-Miller (1986) scheme. Convective heating Q_c is described by:

$$Q_c \propto \tau_c^{-1} \mathcal{H}(C_1) C_1 \quad (1)$$

where τ_c is the convective relaxation timescale (= 2 hrs), $\mathcal{H}(C_1)$ is zero for $C_1 \leq 0$, and one for $C_1 > 0$, and C_1 is a measure of the convective available potential energy (CAPE), projected onto the model’s temperature and moisture basis functions.

In the stochastic convective formulation, a first-order autoregressive (Markov process) random noise component (ξ) is added to the deterministic C_1 calculated from grid-scale temperature and moisture. The Markov process has a characteristic timescale of τ_ξ , and runs are made for $\tau_\xi = 20$ min, 2 hrs, and 1 day. Details are given in Lin and Neelin (2000).

An approximation of the probability distribution function (pseudo-PDF) in a region of frequent tropical convection also shows a strong dependence on autocorrelation time (Figure 3). As autocorrelation time increases, the daily distribution is skewed towards more frequent low precipitation occurrences, resembling more closely the mixed lognormal shape of observed precipitation.

For 850 hPa zonal wind, the inclusion of stochastic convection enhances eastward propagating, low-wave-number, low-frequency variability. Figure 4 shows the spectra for 850 hPa zonal wind wavenumber 1 in an equatorial band for a control run without stochastic convection (dotted line) as well as with stochastic convection (solid lines). At the shorter τ_ξ , the inclusion of stochastic convection produces a substantial response in the 10–40 day range. At $\tau_\xi = 1$ day, the response occurs at even lower frequencies, with a signal peak in the range of 20–40 days. This is a combination of effects due to dry wave dynamics, moist wave dynamics, and autocorrelation in the stochastic process.

4.2 The CCM3 CAPE- M_b and VSH Schemes

An essential postulate of the closure in ZM is that convection tends to remove positive CAPE at a rate proportional to the CAPE so, if acting alone, convection would cause CAPE to decay exponentially on a timescale τ_c . In the CAPE- M_b stochastic closure, we posit that the convective tendency of CAPE $(\partial_t A)_c$ is modified by a stochastic process, ξ :

$$(\partial_t A)_c = -\tau_c^{-1}(A + \xi), \quad (2)$$

for $(A + \xi) \geq 0$, so random variations occur about the ZM exponential decay tendency. The convective CAPE tendency is also obtained from the updraft/downdraft model, which can be expressed as $-M_b F$ where M_b is

(a) January, control run

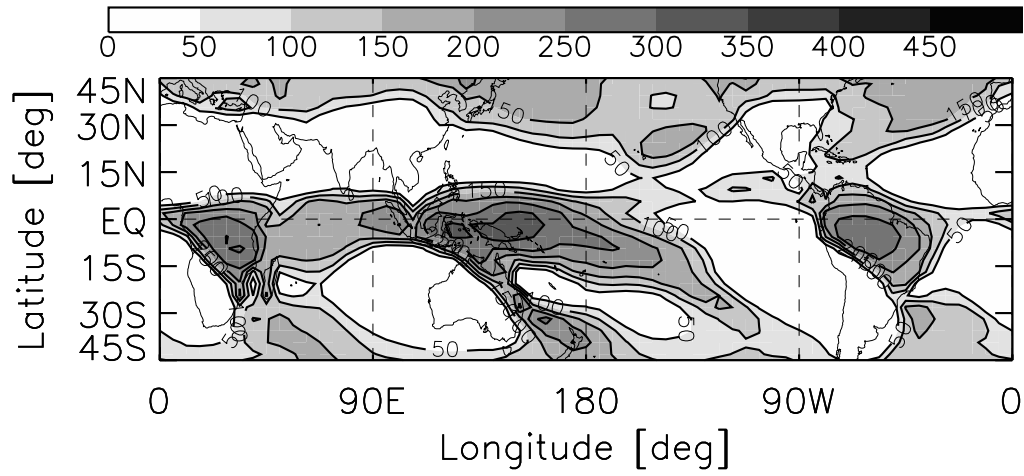
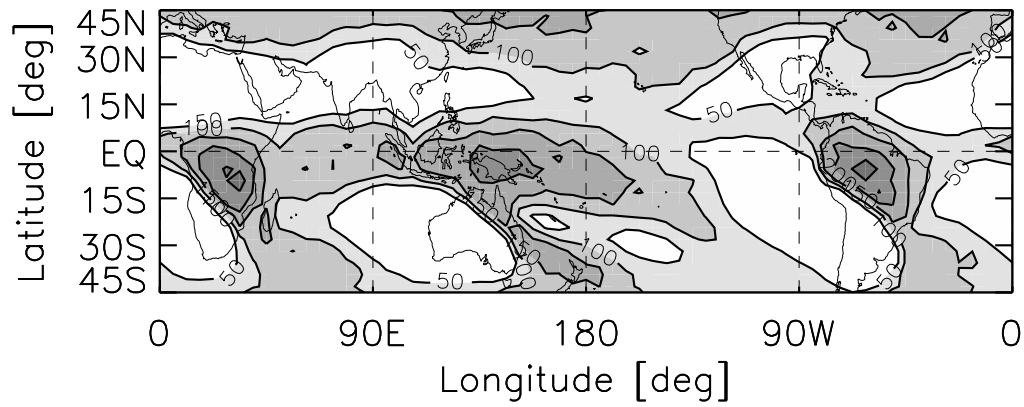
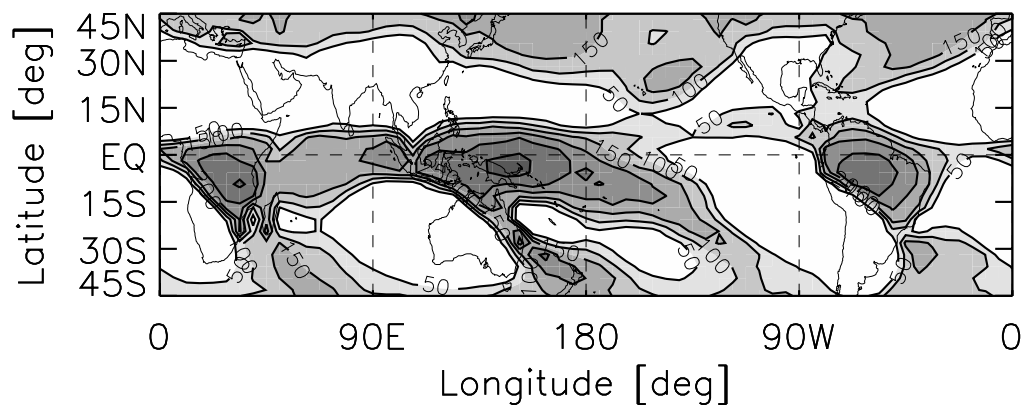

 (b) January, empirical lognormal scheme, $\tau_{\xi} = 1$ day, $\alpha = 1$

 (c) January, empirical lognormal scheme, $\tau_{\xi} = 1$ day, $\alpha = 11$


Figure 2: January precipitation climatology (W m^{-2}) for the (a) control run, (b) empirical lognormal scheme ($\alpha = 1$, $\tau_{\xi} = 1$ day), and (c) empirical lognormal scheme ($\alpha = 11$, $\tau_{\xi} = 1$ day). Contour interval is 50.

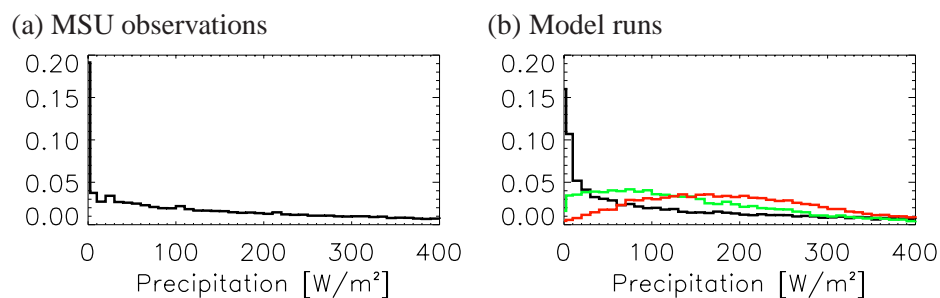


Figure 3: Pseudo-PDF of daily mean precipitation in region of frequent tropical convection for (a) MSU (180–202.5°E, 5°N during the period 1 Jan 1979 to 31 Dec 1995), and (b) model runs (180–202.5°E, 5.625°N for 10 model years). Panel (b) shows $\tau_\xi = 20$ min (red), $\tau_\xi = 2$ hrs (green), and $\tau_\xi = 1$ day (black) model runs. Bin size for both pseudo-PDFs is 10 W m^{-2} .

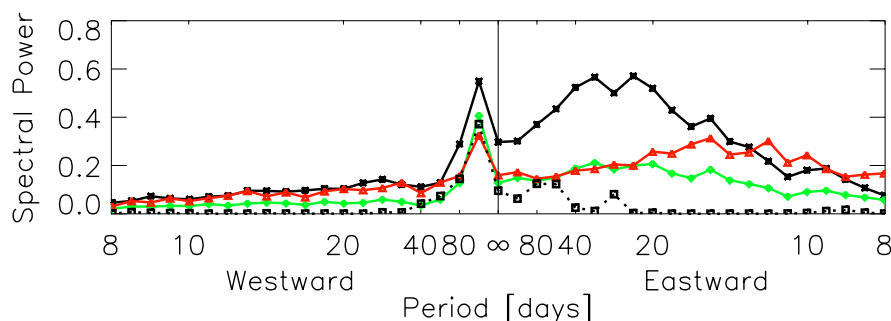


Figure 4: Power spectrum for 850 hPa zonal wind wavenumber 1 of non-areally weighted meridional mean in latitude band from 5.625°N to 5.625°S, for $\tau_\xi = 20$ min (red), $\tau_\xi = 2$ hrs (green), $\tau_\xi = 1$ day (black solid), and control run without stochastic convection (black dotted). Units $(\text{m sec}^{-1})^2$. Standard deviation of spectra is 10%.

the updraft cloud-base mass flux and F is the CAPE tendency per unit M_b . Equating this tendency to that due to the closure (2) yields

$$M_b = \frac{A + \xi}{\tau_c F}, \quad (3)$$

with the additional condition $M_b \geq 0$. The conventional ZM case is simply $\xi = 0$. The introduction of a stochastic element in the CAPE decay closure implies that the cloud base mass flux has random variations.

The CAPE- M_b scheme uses the vertical structure obtained from the conventional ZM scheme, but there is potentially also variability in the vertical structure that should be represented stochastically. Physically, this dependence might correspond, for instance, to differing levels of detrainment for individual convective elements or to differences in squall line organization due to vertical shear. The VSH scheme is a simple way of testing the impacts of random variations in the vertical structure of the heating on large-scale dynamics. In this scheme, at each timestep noise is added directly to the adjustment of temperature at each level by the convective scheme only at locations where ZM deep convection may occur. To help ensure energy conservation, the mass weighted vertical mean of the noise is subtracted at each level.

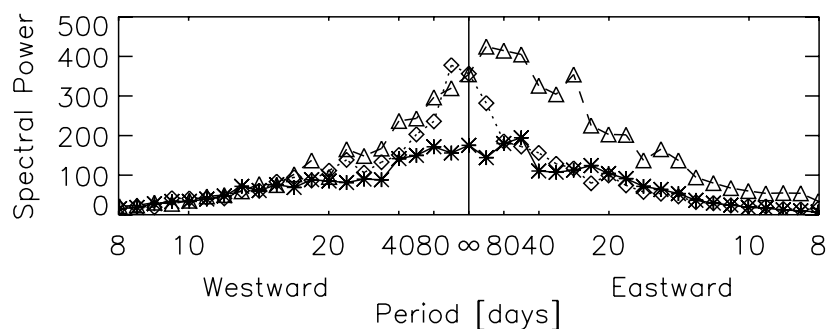


Figure 5: Wavenumber one spectral power of equatorial region 850 hPa zonal wind anomalies for control run (asterisk), CAPE- M_b scheme (diamond), and VSH scheme (triangle). Units (m s^{-1})².

The VSH scheme does not affect precipitation (or vertical mean heating) as calculated by the ZM scheme at any given time step. Thus in principle, any effects of the noise on the precipitation must go through the large-scale dynamics and physics of the rest of the model before they feed back on precipitation. Some variation from this may occur for mid-level and shallow convection since the Hack scheme (Hack 1994) is called subsequent to the ZM scheme.

In both the CAPE- M_b and VSH schemes, the noise added at time t (ξ) has the form of a first-order Markov process with an autocorrelation time τ_ξ . Given the results with the empirical lognormal and CAPE schemes, $\tau_\xi = 1$ day is used in the CAPE- M_b and VSH explorations here. Details of both stochastic schemes are given in Lin and Neelin (2003).

While the CAPE- M_b scheme succeeds in raising tropical daily precipitation variance toward observed (not shown), suggesting that a substantial part of the observed daily variability arises from small scale processes, the CAPE- M_b scheme has little impact on spectral power at low-wavenumbers and low-frequencies (Figure 5). This aspect differs from findings with the CAPE scheme in QTCM1 and may depend on interaction with low frequency variability that exists in the control. The VSH scheme, however, gives selective enhancement of the low-wavenumber and low-frequency power, apparently through dynamical filtering of the response prior to the interaction with cloud-base mass flux and precipitation (Figure 5).

Lag-regression plots of 20–80 day bandpass filtered 850 hPa zonal wind anomalies (Figure 6) for the months of Dec–May, when Madden-Julian oscillation strength is at its highest in the Indian Ocean and western Pacific Ocean (Salby and Hendon 1994), summarize key features of the spatial structure and propagation of the circulation (Maloney and Hartmann 2001). The CAPE- M_b scheme appears to decrease the wavenumber of westward propagating features west of the dateline, but appears to be unable to produce a clear large-scale eastward propagating signal. In contrast, the VSH scheme produces a coherent eastward propagating signal across all longitudes, similar in some ways to reanalyses lag-regression structure (Maloney and Hartmann 2001, Fig. 3a).

5 Conclusions

These results suggest a number of implications for climate modeling. The empirical lognormal example of schemes using the empirical approach indicates heating strongly interacts with the large-scale. As a result, one cannot estimate the PDF of heating from data and then calibrate a stochastic scheme offline, since dynamics so strongly changes the simulated properties. Second, large-scale dynamics tends to adjust the mean towards a climatology intrinsic to the model. Thus, preservation of the mean of the deterministic scheme is not an impor-

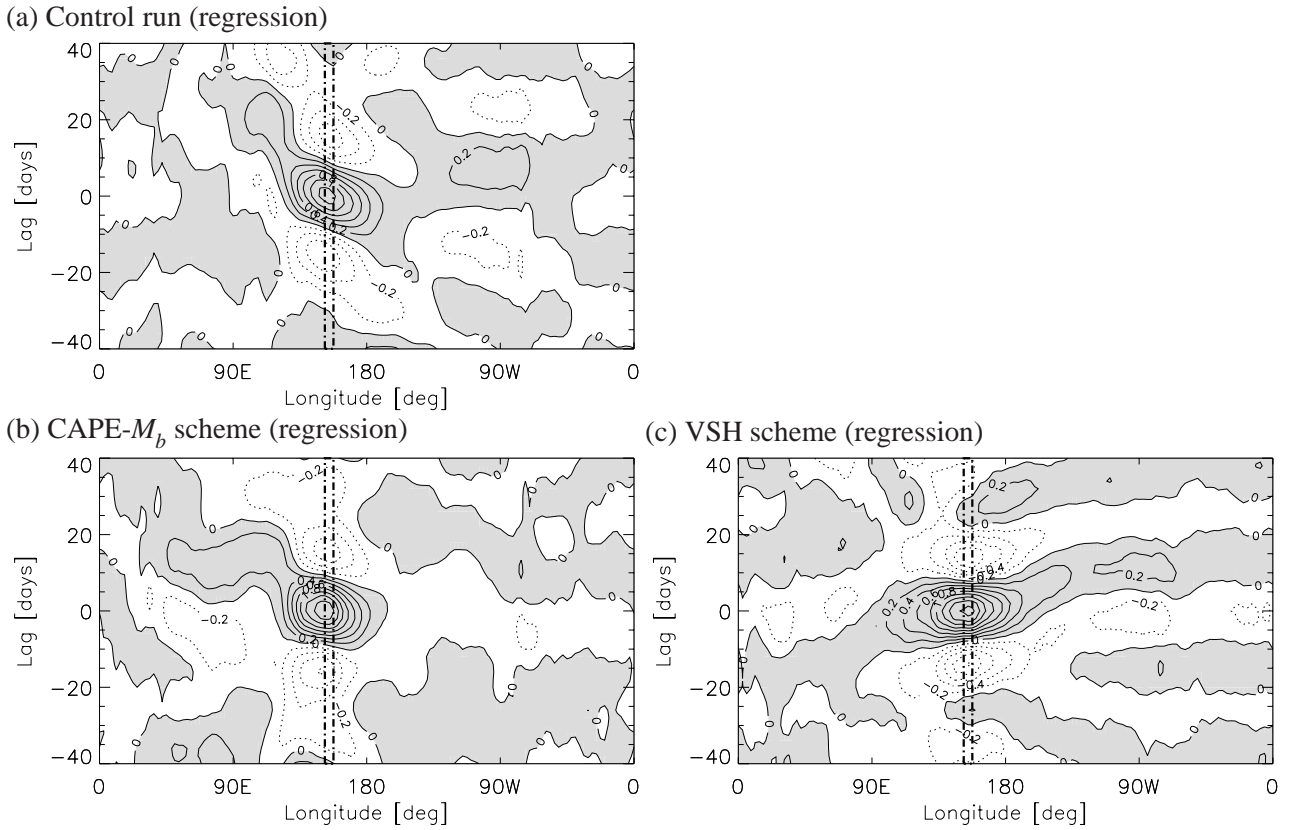


Figure 6: Lag-regression plots of equatorial region 850 hPa zonal wind anomalies ($t + \text{lag}$) regressed to a 850 hPa zonal wind anomaly reference timeseries (t) for the months Dec–May for the (a) control run, (b) CAPE- M_b scheme, and (c) VSH scheme. The reference timeseries is the non-areally weighted mean between 9.8°S – 9.8°N and 151.8 – 157.6°E and its longitude range is indicated by the bold dash-dot line. Units m s^{-1} . Fields are 20–80 day bandpass filtered prior to regression. Non-negative (negative) anomalies are solid (dotted) lines. Positive values are shaded. Contour interval is 0.2.

tant property for a stochastic scheme. Third, intraseasonal variability can be strongly impacted by inclusion of a stochastic component, but there is parameter sensitivity.

The QTCM1 and CCM3 examples of schemes from the physics-motivated approach also suggest while there is parameter sensitivity, even a simple version (e.g., CAPE scheme) can yield encouraging results. Autocorrelation time of the stochastic processes matters, and longer autocorrelation time (order 1 day) yields more impact and better results for the QTCM1 CAPE scheme example, suggesting mesoscale processes may be important. Stochastic forcing arising physically from small-scales can be a significant source of intraseasonal variability, but its nature depends strongly on interaction with the large-scale. For instance, the CAPE- M_b scheme impacts precipitation directly with a signature that is initially spatially white and dynamical feedbacks occur subsequent to this. On the other hand, variations in vertical structure seen in the VSH scheme yield a signature more suggestive of dry wave types. We hypothesize that the dominant pathway for VSH impacts is initiated by the excitation of waves with a spectrum of vertical structures. The fast phase speeds of dry waves acts as a dynamical “pre-filter” that tends to select large spatial structures in the wind and temperature fields, which then impact the precipitation. In that way, the VSH impact may favor selective enhancement of low-wavenumber variability.

Acknowledgments

Lin and Neelin (2002) is copyright by the American Meteorological Society and its use in the present work is by permission of the American Meteorological Society. Lin and Neelin (2000) and Lin and Neelin (2003) are both copyright by the American Geophysical Union and its use in the present work is by permission of the American Geophysical Union. In addition to the acknowledgements in those references, we thank Joyce Meyerson for help in revising figures for the presentation for this workshop. Additional work by JW was carried out at the Climate Systems Center at the University of Chicago, funded by the NSF Information Technology Research Program under grant ATM-0121028.

References

- Betts, A. K. and M. J. Miller, 1986: A new convective adjustment scheme. Part II: Single column tests using GATE wave, BOMEX, ATEX and Arctic air-mass data sets. *Quart. J. Roy. Meteor. Soc.*, **112**, 693–709.
- Bonan, G. B., 1998: The land surface climatology of the NCAR Land Surface Model coupled to the NCAR Community Climate Model. *J. Climate*, **11**, 1307–1326.
- Eagleson, P. S., 1978: Climate, soil, and vegetation: 2. The distribution of annual precipitation derived from observed storm sequences. *Water Resour. Res.*, **14**, 713–721.
- Hack, J. J., 1994: Parameterization of moist convection in the National Center for Atmospheric Research Community Climate Model (CCM2). *J. Geophys. Res.*, **99**, 5551–5568.
- Kedem, B., L. S. Chiu, and G. R. North, 1990: Estimation of mean rain rate: Application to satellite observations. *J. Geophys. Res.*, **95**, 1965–1972.
- Kiehl, J. T., J. J. Hack, G. B. Bonan, B. A. Boville, D. L. Williamson, and P. J. Rasch, 1998: The National Center for Atmospheric Research Community Climate Model: CCM3. *J. Climate*, **11**, 1131–1149.
- Lin, J. W.-B. and J. D. Neelin, 2000: Influence of a stochastic moist convective parameterization on tropical climate variability. *Geophys. Res. Lett.*, **27**, 3691–3694.
- Lin, J. W.-B. and J. D. Neelin, 2002: Considerations for stochastic convective parameterization. *J. Atmos. Sci.*, **59**, 959–975.
- Lin, J. W.-B. and J. D. Neelin, 2003: Towards stochastic deep convective parameterization in general circulation models. *Geophys. Res. Lett.*, **30**, 1162, doi:10.1029/2002GL016203.
- Maloney, E. D. and D. L. Hartmann, 2001: The sensitivity of intraseasonal variability in the NCAR CCM3 to changes in convective parameterization. *J. Climate*, **14**, 2015–2034.
- Neelin, J. D. and N. Zeng, 2000: A quasi-equilibrium tropical circulation model—formulation. *J. Atmos. Sci.*, **57**, 1741–1766.
- Salby, M. L. and H. H. Hendon, 1994: Intraseasonal behavior of clouds, temperature, and motion in the Tropics. *J. Atmos. Sci.*, **51**, 2207–2224.
- Spencer, R. W., 1993: Global oceanic precipitation from the MSU during 1979–91 and comparisons to other climatologies. *J. Climate*, **6**, 1301–1326.
- Zeng, N., J. D. Neelin, and C. Chou, 2000: A quasi-equilibrium tropical circulation model—implementation and simulation. *J. Atmos. Sci.*, **57**, 1767–1796.
- Zhang, G. J. and N. A. McFarlane, 1995: Sensitivity of climate simulations to the parameterization of cumulus convection in the Canadian Centre general circulation model. *Atmos.-Ocean*, **33**, 407–446.